Chapter 8

Fourier Transform Infrared Spectroscopy for Molecular Analysis of Microbial Cells

Jesús J. Ojeda and Maria Dittrich

Abstract

A rapid and inexpensive method to characterise chemical cell properties and identify the functional groups present in the cell wall is Fourier transform infrared spectroscopy (FTIR). Infrared spectroscopy is a well-established technique to identify functional groups in organic molecules based on their vibration modes at different infrared wave numbers. The presence or absence of functional groups, their protonation states, or any changes due to new interactions can be monitored by analysing the position and intensity of the different infrared absorption bands. Additionally, infrared spectroscopy is non-destructive and can be used to monitor the chemistry of living cells. Despite the complexity of the spectra, the elucidation of functional groups on Gram-negative and Gram-positive bacteria has been already well documented in the literature. Recent advances in detector sensitivity have allowed the use of micro-FTIR spectroscopy as an important analytical tool to analyse biofilm samples without the need of previous treatment. Using FTIR spectroscopy, the infrared bands corresponding to proteins, lipids, polysaccharides, polyphosphate groups, and other carbohydrate functional groups on the bacterial cells can now be identified and compared along different conditions. Despite some differences in FTIR spectra among bacterial strains, experimental conditions, or changes in microbiological parameters, the IR absorption bands between approximately 4,000 and 400 cm^{-1} are mainly due to fundamental vibrational modes and can often be assigned to the same particular functional groups. In this chapter, an overview covering the different sample preparation protocols for infrared analysis of bacterial cells is given, alongside the basic principles of the technique, the procedures for calculating vibrational frequencies based on simple harmonic motion, and the advantages and disadvantages of FTIR spectroscopy for the analysis of microorganisms.

Key words: Bacteria, Biofilm, Cell surface, In situ analysis, Fourier transform infrared spectroscopy, Attenuated total reflectance, ATR-FTIR, Micro-FTIR, Vibrational spectroscopy.

1. Introduction

The use of Fourier transform infrared spectroscopy (FTIR) as an analytical tool to describe and monitor the chemical changes and physiology of bacterial cells has become an increasingly popular choice, and is now a routine protocol in many microbiological applications. The use of infrared spectroscopy for the analysis of

Ali Navid (ed.), *Microbial Systems Biology: Methods and Protocols*, Methods in Molecular Biology, vol. 881,
DOI 10.1007/978-1-61779-827-6_8,

biological samples was first suggested by William Weber Coblentz in 1911 (1), and a subsequent paper by Stair and Coblentz in 1935 explored the infrared absorption spectra of different plant and animal tissues (2). In the 1950s, Randall, Smith and collaborators actively pursued the use of infrared spectroscopy to differentiate and correlate the biological properties of the strains of *Mycobacterium* with their infrared spectra (3–6), while K.P. Norris and Randall et al. also maintained an active interest in the use of infrared spectroscopy and its application to microbiology, especially for bacterial identification (7, 8). However, the lack of spectral analysis tools and instrumental limitations made difficult the establishment of infrared spectroscopy as a regular practice for the analysis of microorganisms (9).

The improvement of modern interferometers and the development of FTIRs in the 1980s prompted anew the interest in the application of the technique for biological materials (9–11). In the 1990s, Naumann and collaborators were able to study bacterial cells in situ, and developed methods for the analysis of complex infrared data to differentiate and classify bacteria (9, 10, 12, 13).

Commercially available since the 1995s, the new FTIR microspectrometers allowed chemical imaging capabilities, due to the migration from single-element detectors to focal plane array (FPA) detectors and the development of mercury–cadmium–telluride IR arrays. This new advance in instrumentation has already been applied to a variety of microbiological studies for the identification of various bacteria and the chemical composition of biofilms in a wide variety of matrixes (14–21), and has enormously increased the interest of FTIR spectroscopy for the analysis of microorganisms (9).

1.1. Infrared Spectroscopy

Infrared spectroscopy is a well-established technique to identify the functional groups in a molecule based on its vibration modes at different infrared frequencies. The term "infrared" covers the range of the electromagnetic spectrum between 0.78 and 1,000 μm (22). In the context of infrared spectroscopy, wavelength is measured in "wavenumbers", as units cm^{-1}. Absorption of infrared radiation by a typical organic molecule will result in the excitation of vibrational, rotational, and bending modes.

For simple systems, the atoms in a molecule can be considered as point masses, linked by a "spring." To absorb infrared radiation, the molecule must cause a net change in the dipole moment as it vibrates. Under these circumstances, the alternating electrical field of the radiation will interact with the fluctuations in the dipole moment of the molecule. If the frequency of the radiation matches the natural vibrational frequency of the molecule, then the radiation will be absorbed, producing a change in the amplitude of molecular vibration (22).

Molecular vibrations fall into two main categories: stretching or bending. The stretching vibration entails a change in the

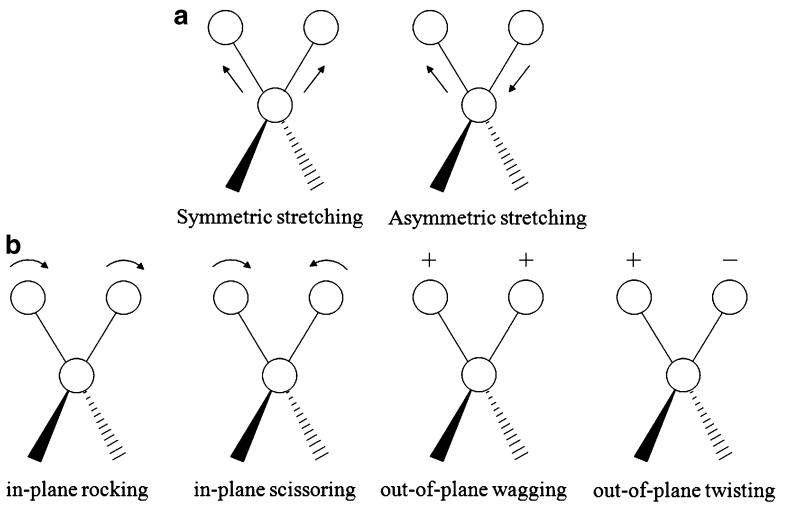

Fig. 1. Types of molecular vibrations: (**a**) Stretching vibrations and (**b**) bending vibrations. "+" and "−" symbols indicate motion towards the paper and away from the paper, respectively.

inter-atomic distance along the bond axis, whereas in bending vibrations the bond lengths remain constant, but the bond angles change. There are four types of bending vibrations: rocking, scissoring, wagging, or twisting (Fig. 1) (22). Stretching absorptions usually produce stronger peaks than bending in the infrared spectrum; however, bending absorptions can be useful in differentiating similar types of bonds.

By imaging the atoms in a molecule as masses connected by a spring, the displacement of one of these masses from its equilibrium by a distance x will generate a restoring force F proportional to the displacement. This restoring force can be described by the Hooke's Law as:

$$F = -k \times x$$

where k is the force constant of the spring.

If we describe the force F in terms of Newton's second law:

$$F = m \times a$$

where m is a mass in motion and a is its acceleration, the two equations can be combined as:

$$m \times a = -k \times x.$$

Because a is the second derivative of the distance (x) with respect to time (t), the above equation can be re-written as:

$$m\frac{\mathrm{d}^2x}{\mathrm{d}t^2} = -kx$$

The solution of this differential equation is:

$$x = x_o \sin(2\pi v_{osc} t + \phi)$$

where v_{osc} is the vibrational frequency of the oscillation, x_o is the maximum amplitude of the movement and ϕ is a phase constant dependent on the initial conditions. The second derivative of x will then be given by:

$$\frac{d^2x}{dt^2} = -4\pi^2 v_{osc}^2 x_o \sin(2\pi v_{osc} t + \phi)$$

and therefore,

$$\begin{aligned} m\frac{d^2x}{dt^2} = -kx \Rightarrow m[-4\pi^2 v_{osc}^2 x_o \sin(2\pi v_{osc} t + \phi)] \\ = -k[x_o \sin(2\pi v_{osc} t + \phi)] \end{aligned}$$

Rearranging:

$$\frac{m}{k} = \frac{x_o \sin(2\pi v_{osc} t + \phi)}{4\pi^2 v_{osc}^2 x_o \sin(2\pi v_{osc} t + \phi)}$$

$$\frac{m}{k} = \frac{1}{4\pi^2 v_{osc}^2}$$

$$v_{osc} = \tfrac{1}{2\pi}\sqrt{\tfrac{k}{m}}$$

In the above equation, the vibration of the atoms has been reduced to the vibration of a single mass m, the "effective" inertial mass or "reduced mass" of the system. In order to describe the behaviour of a system containing two masses m_1 and m_2 connected by a spring, the reduced mass needs to be substituted as follows:

$$m_{red} = \mu = \frac{m_1 m_2}{m_1 + m_2}$$

Therefore, the vibrational frequency of two atoms linked by a "spring" having a force constant k is given by the equation:

$$v_{osc} = \frac{1}{2\pi} = k\sqrt{\frac{m_1 + m_2}{m_1 m_2}}$$

It should be remembered that a linear wavenumber scale is preferred in infrared spectroscopy, and the relationship between wavenumber ($\bar{v}$) and frequency (v) is given by:

$$\bar{v}(\mathrm{cm}^{-1}) = \frac{v(\mathrm{Hz})}{c(\mathrm{cm/s})}$$

where c is the velocity of light. Therefore, the frequency of infrared light absorbed by a molecule consisting of two atoms, in wavenumbers, is given by:

$$\bar{v} = \frac{1}{2\pi c}\sqrt{k\frac{m_1 + m_2}{m_1 m_2}}$$

where:

k = force constant of the bond (in N/m)
c = speed of light (in cm/s)
m_1 and m_2 are the masses of the two atoms (in kg)

Generally, k can be assumed to be around 5×10^2 N/m for single bonds (e.g., C–H, O–H), 1×10^3 N/m for double bonds (e.g., C=O, C=C), and 1.5×10^3 N/m for triple bonds (e.g., C≡N, C≡C) (22).

This equation can be used to estimate the wavenumber of the fundamental absorption band due to the stretching vibration for a variety of bond types. By looking at this equation, it can be inferred that if there is a high value of k (i.e. the bond is strong), the bond will absorb at higher wavenumbers; for example, C=C double bond would absorb at higher wavenumbers than a C–C single bond. In addition, the larger the two masses, the lower the wavenumber. Although simple in concept, there is a reasonably good fit between the stretching vibrations predicted and the values observed experimentally (23).

Having defined the basis for the simple vibration of an atomic bond, it is necessary to look at complex molecules that may contain several types of atoms as well as bonds. In a polyatomic molecule, each atom can be located as a point in the space with coordinated x, y, and z. For an N number of atoms, a total of $3N$ coordinates will be required. There is one degree of freedom per independent mode of motion. Therefore, each coordinate corresponds to one degree of freedom, and hence, for a molecule containing N atoms, it is said that it contains $3N$ degrees of freedom. However, not all of these correspond to vibration modes. The rotational motion of the molecule around its centre of gravity requires three coordinates; and the translational motion of its centre of gravity requires another three degrees of freedom. The remaining $3N - 6$ degrees of freedom represent the number of possible vibrations within the molecule (22–24). In general, any molecule with more than two atoms has six degrees of rigid motion freedom, one degree of bond length vibrational freedom for every bond, and one degree of bond angle vibrational freedom for every atom connecting two other atoms. For a linear molecule, the rotational motion can be described by two degrees of freedom instead of three (because the rotation about the bound axis is not possible) and thus, for a linear molecule the number of vibrations is $3N - 5$.

In practice, with the exception of the simplest of compounds, most molecules have nonlinear structures (apart from where a

specific functional group or groups generate a predominant linear arrangement). However, if the number of modes of vibration for a simple hydrocarbon such as methane is calculated (5 atoms, tetrahedral structure); a value of nine is obtained. This would imply that nine sets of absorption frequencies would be observed in the infrared spectrum of methane gas. In fact, the number observed is far less, corresponding to the asymmetric and symmetric stretching and bending of the C–H bonds about the central carbon atom (23). The reason for producing fewer experimental bands than would be expected is usually because some of the vibrations could be redundant or degenerate (that is to say, the same amount of energy is required for these vibrations). Other reasons that can be attributed to the observation of less experimental bands than the theoretical number of normal modes are that no changes in dipole moments resulted from a specific vibration, or that the absorption intensity was too low to be detected by the instrument, or that the vibrational energy was in a wavelength region beyond the range of the spectrometer (22, 23).

In addition to the stretching and bending vibrations, interaction between vibrations can occur (coupling) if the vibrating bonds are joined to a single, central atom. This will influence the energy of the vibration and the wavelength of the corresponding absorption (22). Vibrational coupling is influenced by a number of factors (22):

1. When there is a common atom between the two vibrating bonds, strong coupling of stretching vibrations will occur.
2. When there is a common bond between vibrating groups, coupling of bending vibrations will occur.
3. If the stretching bond is on one side of an angle varied by a bending vibration, coupling between a stretching vibration and a bending vibration will occur.
4. When the coupled groups have approximately equal energies, coupling will be greatest.
5. If the groups are separated by two or more bonds, no coupling will be seen between them.

As mentioned before, in order for a vibrational mode in a molecule to be infrared active, it must be associated with changes in the permanent dipole. When an infrared light interacts with the matter, the chemical bonds will stretch, contract, or bend. Weaker bonds will require less energy to vibrate whereas stronger bonds will need more energy; therefore, the frequency of the vibrations can be associated with a particular bond type, as each functional group will have its own characteristic vibrational frequency.

The presence or absence of functional groups, its protonation states, or any changes due to new interactions can be monitored by analysing the position and intensity of the different infrared

absorption bands. If there are more atoms, there will be more bonds, and hence, more modes of vibrations that will result in a more complicated spectrum. However, in the case of bacterial samples, despite the complexity of the infrared spectra, the elucidation of functional groups has been already well established (9, 10, 12, 17, 22, 24–31). Additionally, IR spectroscopy is non-destructive and can be used to monitor the chemistry of living cells as well.

The infrared spectrum is measured by calculating the intensity of the infrared radiation before and after passing through the sample. The percentage of transmittance ($\%T$) can be defined as:

$$\%T = \frac{I}{I_o}$$

where I_o is the intensity of the infrared beam before passing though the sample and I is the intensity of the beam after passing through the sample.

The absorbance (A) can be calculated from the transmittance spectrum using the following equation:

$$A = -\log T = \log \frac{1}{T}$$

For quantitative analysis, absorbance spectra are commonly used. According to the Beer's law, if the absorbance (A), path length (d), and the molar absorptivity (ε) are known, the concentration (c) of the substance can be deduced based on the equation:

$$A = \varepsilon c d$$

The final infrared spectrum (in either absorbance or transmittance) should be absent of all instrumental and environmental contributions, and only present the features of the sample. Therefore, a background spectrum should be taken beforehand, and the final spectrum should be the result of the sample single beam normalised against the background (9, 24, 32).

1.2. Instrumentation

Early studies of infrared spectroscopy of bacteria were made with dispersive-type infrared spectrometers, but since 1980 they were made almost exclusively with Fourier Transform infrared spectrometers, due to the advantages they offer. Figure 2 shows the basic components of these spectrometers, and schematically shows how to generate the spectroscopic information.

Radiation from a polychromatic source collides into a beam splitter and is divided into two beams: one of them is reflected to a fixed mirror while the other is reflected to a moving mirror (the exact position of this movable mirror is measured with a mini-laser on the internal compartment of the instrument). After being reflected at each mirror, the beam recombines, producing constructive or destructive interference depending on the separation distance between the movable mirror and the static mirror. This process

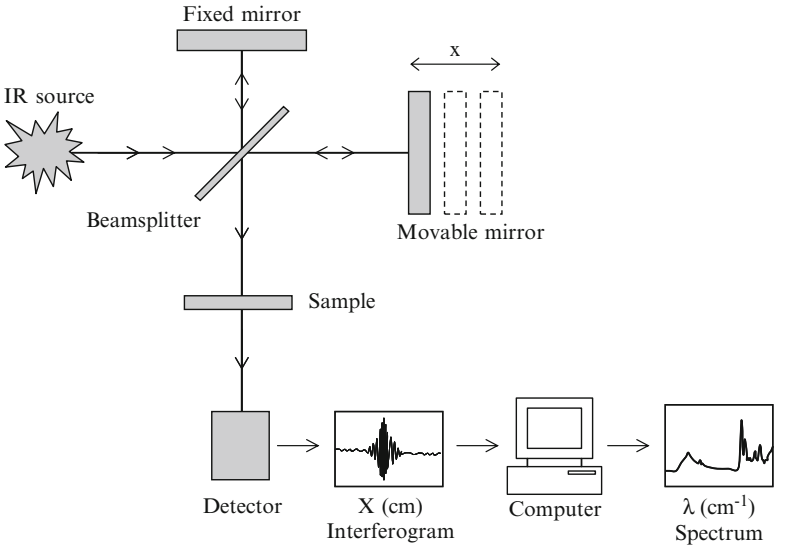

Fig. 2. Schematic sketch of the essential features of a Fourier transform infrared (FTIR) spectrometer.

produces again two beams: one returning back to the source of power and the other that goes towards the sample and is measured by the detector. This information accumulates as an interferogram in the memory of the computer. Due to the speed (usually less than 1 s) and high-accuracy throughout the process, hundreds or thousands of interferograms can be accumulated, and then added and converted through a Fourier transform in a conventional transmittance (or absorbance) spectra against wavenumbers (33).

According to Burgula et al., Naumann et al., and Mariey et al., (9, 10, 12, 29) the following could be considered as advantages and disadvantages of FTIR spectroscopy for the analysis of microorganisms:

Advantages:

- Provides information related to the molecular properties of the sample.
- Relative fast technique (most samples can be scanned in about 5 min).
- Usually requires little sample (milligrams or micrograms in case of micro-FTIR).
- A high signal-to-noise ratio can be achieved.
- Non-destructive technique.
- The use of algorithms for data analysis, such as principal component analysis (PCA), has been successfully applied to allow the identification of key chemical moieties that distinguish between different strains (34–37).

Disadvantages:

- Spectral analysis is based on very specific regions, and the presence of water may interfere in these regions.
- It requires expertise in the analysis of the spectra.
- FTIR spectroscopy does not detect elements or diatomic molecules (such as N_2 or O_2).
- Spectral regions of various components often overlap, leading to incorrect interpretation of the results.
- Microbiological media parameters, such as culture medium, growth temperature, or growth time may cause differences in the spectra obtained. However, this could also be considered an advantage, as it can allow detecting the impact of different conditions in the bacterial physiology.

1.3. Interpretation of FTIR spectra

Figure 3 presents a typical FTIR spectrum of bacterial cells, in this case Gram-negative *Pseudomonas putida* ATCC 11172. The sample consisted of a suspension of cells that were let to dry under gentle N_2 flow on the top of a Germanium ATR crystal. The observed infrared bands of the spectra correspond to the presence of proteins, lipids, polysaccharides, polyphosphate groups, and other carbohydrate functional groups. The functional groups assigned to the infrared bands and the corresponding frequencies for the sample are summarised in Table 1.

The region between 3,000 and 2,800 cm^{-1} shown in Fig. 3 exhibited the typical C–H stretching vibrations (ν_{C-H}) corresponding to the CH_3 and $>CH_2$ functional groups, present in fatty acids and lipids (2,850 cm^{-1}). The O–H stretching signal

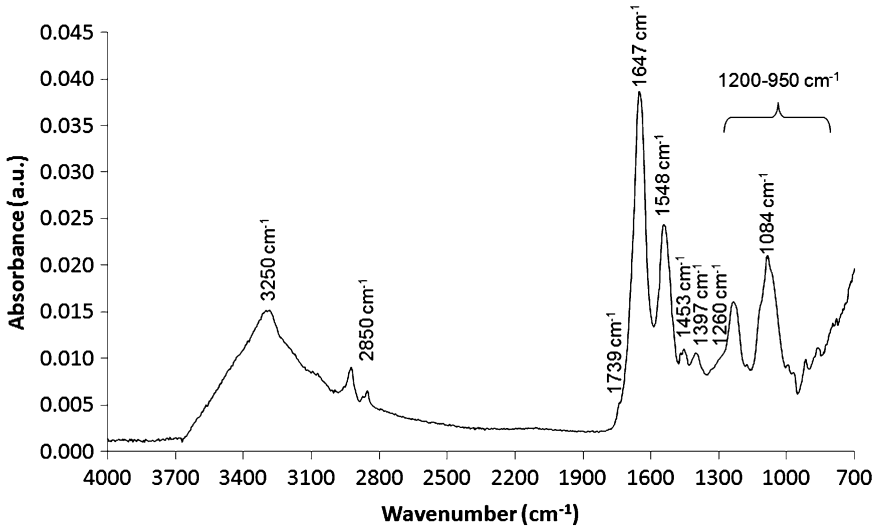

Fig. 3. Typical FTIR spectrum of a bacterial sample (*Pseudomonas putida* ATCC 11172).

Table 1
Infrared absorption bands of the most common bacterial functional groups

Wavenumber (cm^{-1})	Functional group assignment[a]
1,739	Stretching C=O of ester functional groups from membrane lipids and fatty acids; stretching C=O of carboxylic acids
1,647	Stretching C=O in amides (amide I band)
1,548	N–H bending in amides (amide II band)
1,405	Symmetric stretching for deprotonated COO^- group
1,453	C–N stretching in amides (amide III band)
1,397	Symmetric stretching of COO^-; Bending CH_2/CH_3
1,305	Vibration C–N from amides
1,300–1,250	Vibrations of C–O from esters or carboxylic acids
1,262	Vibrations of –COOH and C–O–H; Double bond stretching of >P=O of general phosphoryl groups and phosphodiester of nucleic acids
1,225	Stretching of P=O in phosphates
1,200–950	Asymmetric and symmetric stretching of PO_2^- and $P(OH)_2$ in phosphates; vibrations of C–OH, C–O–C and C–C of polysaccharides
1,084	Stretching P=O of phosphodiester, phosphorylated proteins, or polyphosphate products
976	Symmetric stretching vibration of phosphoryl groups

[a]Based on Dittrich et al. (25), Jiang et al. (26), Ojeda et al. (17, 27), Schmitt et al. (30), Yee et al. (31), Conley (24), and Wade (28)

(ν_{O-H}) corresponding to the presence of hydroxyl groups can be observed as a broad band around 3,250 cm^{-1}.

The bands around 1,647 and 1,548 cm^{-1} are called amide I and amide II bands, respectively, the former due to stretching C=O ($\nu_{C=O}$) of amides associated with proteins and the latter a combination of bending N–H (δ_{N-H}) of amides. The peak around 1,453 cm^{-1} corresponds to the amine III group (ν_{C-N}) and the peak around 1,397 cm^{-1} can be attributed to the symmetric stretching C–O of carboxylate groups (ν_{COO^-}). Complementary information to support the presence of the C–H peaks can be found in the region between 1,470 and 1,300 cm^{-1}, where bending vibrations of C–H, $>CH_2$ and $-CH_3$ groups takes place. The signal around 1,739 cm^{-1} is actually a combination of two peaks: a signal corresponding to the vibrational C=O stretching ($\nu_{C=O}$) of carboxylic acids at 1,739 cm^{-1} and another peak at 1,725 cm^{-1} corresponding to the stretching C=O of ester functional groups from membrane lipids and fatty acids.

The double bond stretching of >P=O of general phosphoryl groups and phosphodiester of nucleic acids is observed in Fig. 3 at 1,260 cm^{-1}. Vibrations of –COOH and C–O–H are located here as well. The stretching of P=O groups of polyphosphate products, nucleic acid phosphodiester, and phosphorylated proteins is present around 1,084 cm^{-1}. The region between 1,200 and 950 cm^{-1} shows the C–O–C and C–O–P stretching of diverse polysaccharides groups and is usually called the "polysaccharide region."

1.4. IR Techniques

FTIR analysis of microorganisms has been commonly carried out as liquid suspensions in a flow cell device; as biofilms on the top of an attenuated total reflectance (ATR) crystal; freeze-dried, mixed with an alkali halide powder (such as potassium bromide, KBr) and moulded onto a pellet; or using micro-FTIR spectroscopy to obtain a chemical map of a specific area.

In the past, the most common method to analyse bacterial cells was by forming KBr pellets (9, 38). The bacterial samples were freeze-dried, and then grounded carefully onto a fine powder, mixed with KBr, and pressed to form a transparent pellet. Naumann et al. (13, 39) replaced this method with the application of a specialized cuvette for ATR analysis. In this procedure, small amounts of late-exponential-phase cells were removed with a platinum loop from of the agar and suspended in distilled water. An aliquot was then transferred to a ZnSe (zinc selenide) optical plate and dried under moderate vacuum to a transparent film.

In ATR-FTIR spectroscopy, the infrared beam is directed onto a crystal with a high refractive index at a certain angle. Due to the high reflectance index, the infrared beam is totally reflected at the crystal–sample interface. However, this internal reflectance creates an evanescent wave that extends beyond the surface of the crystal into the sample. With ATR spectra, the infrared radiation penetrates only a few micrometres of the sample. The effective penetration depth, d_p, depends on the wavelength of the infrared radiation, the angle of incidence, and the refractive indices of the sample and the ATR crystal (22). The penetration depth can be calculated from the equation:

$$d_p = \frac{\lambda_c}{2\pi\left[\sin^2\theta - (n_s/n_c)^2\right]^{1/2}}$$

where θ is the angle of incidence, λ_c is the wavelength of the beam, and n_s and n_c are the refractive indices of sample and the ATR crystal, respectively. For bacterial cells, the refractive index is assumed to be around 1.39 (26, 40). Therefore, for example, the penetration depth for bacterial cells using a Germanium ATR crystal (refractive index = 4) at an angle of incidence of 60° is around 188 nm at 1,800 cm^{-1} (26).

ATR-FTIR analysis is essentially a surface-sensitive technique. Nevertheless, it should be noted that the average thickness of bacterial cell walls ranges from 20 to 50 nm (26, 41). Consequently, the evanescent wave should penetrate the interior of the bacterial cells, and a contribution from the interior of the cells can also be expected on the ATR-FTIR spectra. However, a study made by Jiang et al. (26), comparing the spectra of isolated cell wall fragments of both Gram-positive and Gram-negative bacteria with the intact cells, showed that the ATR-FTIR spectra of the intact bacterial cells mostly reflected the features of the isolated cell walls.

When a bacterial suspension is placed on the ATR crystal surface, some cells may be in contact with the crystal, while water layers will separate others. The effective penetration depth calculated above is valid for the cells in direct contact with the ATR crystal only (26). Additionally, the uncertainty of refractive indices for bacterial cells, the macromolecular structure of its components, and their variation with solution composition will significantly alter the theoretical penetration depth (26).

Bouhedja et al. (42) used ATR-FTIR to analyse *Escherichia coli* K12 strains by harvesting them from the agar plates with a sterile polystyrene loop, and homogeneously spreading them to cover the whole ATR crystal surface. Another methodology applied by Orsini et al. (18) consisted of transferring microcolonies of *Candida albicans* from the agar plate onto a ZnSe window, by placing the window on the agar plate, and applying a light pressure manually.

The use of liquid flow cells for the analysis of bacterial cells in transmission or reflectance mode, as opposed to ATR-FTIR, has been reported less frequently (27, 43, 44) mainly because water strongly absorbs in the mid-IR light, obscuring the IR signals when present even in a thin layer (43). Therefore, the major challenge using a liquid flow cell is to obtain the optical thickness of water enough to support life and ensure the validity of cells in biofilms, but without masking the bands of interest (43).

FTIR microspectroscopy is a novel tool that combines the FTIR spectroscopy with microscopy (14). Using micro-FTIR spectroscopy, infrared bands can be identified and compared along different microorganisms even without the need to produce a pure culture (10, 18–21). Micro-FTIR analyses of bacteria can be performed either in transmission or reflectance mode. Transmission mode gives high-quality spectra but requires infrared transparent surfaces and transfer of the colonies from the agar plate (16, 18, 21), whereas reflectance micro-FTIR is a convenient tool for the study of biofilm in opaque solid surfaces (17).

Figure 4 shows an example of the application of micro-FTIR spectroscopy for the study of *Aquabacterium commune* biofilm on stainless steel pipes (17). Under the optical microscope, the biofilm looked like a diffuse dark area deposited on the stainless steel surface (Fig. 4a). However, when the sample was irradiated using IR light,

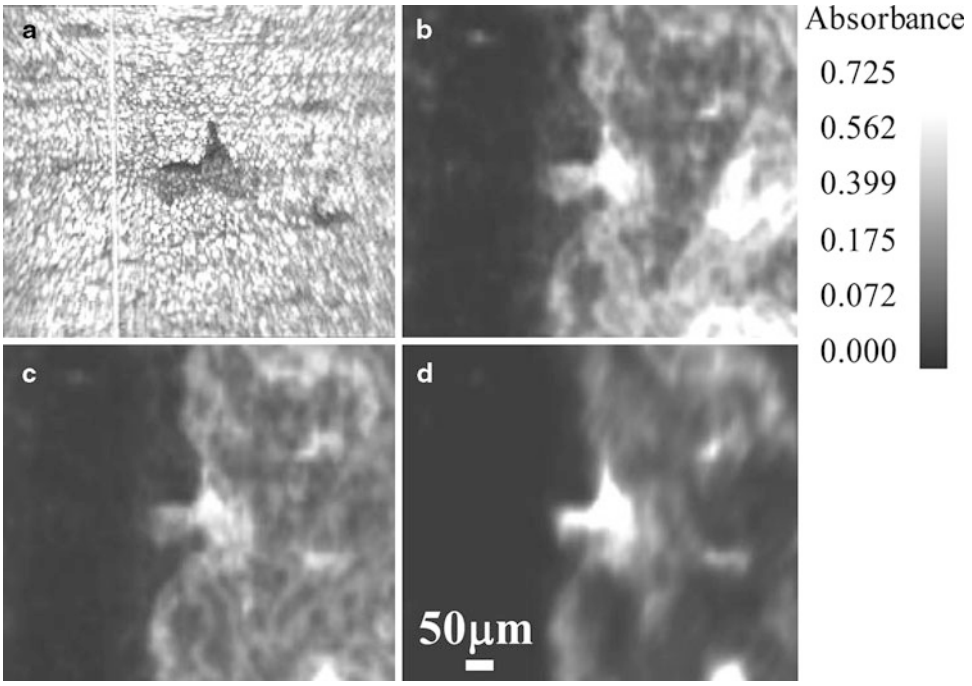

Fig. 4. Application of reflectance micro-FTIR spectroscopy for the study of biofilm formation of *Aquabacterium commune* on stainless steel. (**a**) Optical image of stainless steel and *Aquabacterium commune* biofilm. (**b**) False-grayscale image showing the location of molecules with absorption bands intrinsic of amide I and II (3,550–3,200 and 1,690–1,540 cm^{-1}). (**c**) False-grayscale image showing the location of molecules with absorption bands intrinsic of hydroxyl groups (3,600–3,200 cm^{-1}). (**d**) False-grayscale image showing the location of molecules with absorption bands intrinsic of phosphorylated proteins, polyphosphates, and phosphodiester groups (1,270–1,220, 1,100–1,070 and 1,000–950 cm^{-1}) (adapted with permission from Ojeda et al. (17). Copyright 2009 American Chemical Society).

the image obtained in Fig.4b–d showed the presence of different infrared absorbing molecules. Not all the species absorbing infrared radiation corresponded to *A. commune* cells, but may also come from organic molecules released by the bacterium itself (17).

The areas showing infrared absorption bands intrinsic of amide groups (3,550–3,200 and 1,690–1,620 cm^{-1}) (22, 24–28, 30, 31) are displayed in Fig. 4b. These bands are associated with proteins and are ubiquitous in every FTIR spectra of bacterial cells (9, 25, 26, 30, 31). The release of molecules due to cell lyses or the secretion of extracellular polymeric substances (EPS) could also give signal in this region. Figure 4c shows the presence of hydroxyl groups (associated to polysaccharides and sugars) and Fig. 4d shows the presence of phosphorylated groups (such as phospholipids and phosphodiesters associated with nucleic acids) (17). It seems from these figures that the phosphorylated compounds, sugars, and polysaccharides were covering a rather larger area on the stainless steel than what could be attributed to bacterial cells. This could be because EPS is also formed by phospholipids and phosphate groups liberated during nucleic acid degradation (17, 45).

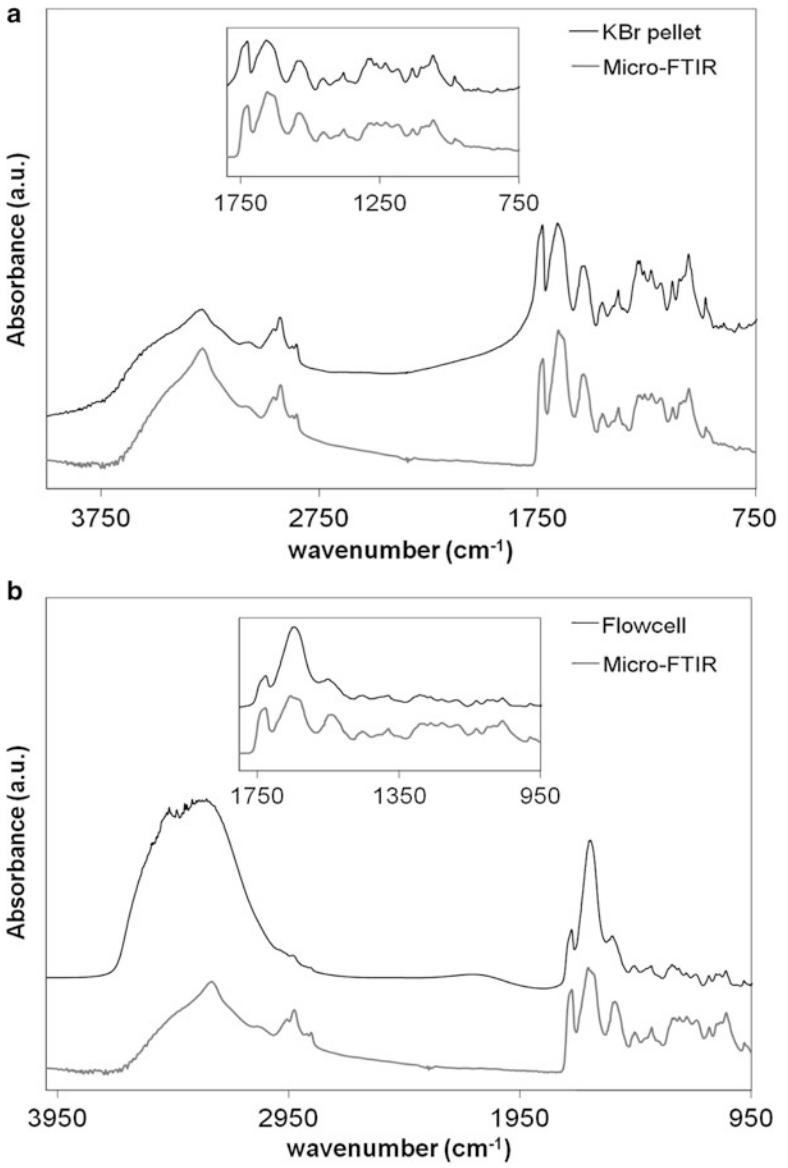

Fig. 5. Comparison between infrared spectra of *Aquabacterium commune* (**a**) using reflectance micro-FTIR and KBr pellet of air-dried samples, and (**b**) using reflectance micro-FTIR and a liquid flow cell (REPRINTED with permission from Ojeda et al. (17). Copyright 2009 American Chemical Society).

Micro-FTIR compares very well with more conventional FTIR techniques, such as transmission, attenuated transmitted reflectance (ATR-FTIR), and KBr pellets, and was found to be a very convenient and precise analytical tool for biofilm analysis. Figure 5 shows a comparison of the spectra obtained when using reflectance micro-FTIR, freeze-dried bacteria prepared on a KBr pellet and live bacterial suspensions scanned using a liquid IR flow cell with CaF_2 windows.

It can be observed that the spectra obtained with any of these techniques produce equivalent results, and no shift was observed in any of the absorption bands. The main difference between the spectra obtained by reflectance micro-FTIR and the liquid flow cell (Fig. 5b) is the presence of a broad band around 3,000 cm^{-1} due to the OH stretching of the water molecules in the flow cell. Additionally, the band appearing at 1,647 cm^{-1} (amide I band) also shows contributions from OH bending vibrations because of the presence of water molecules when using the liquid flow cell.

Previous studies using ATR-FTIR and transmission FTIR have shown that different bacterial cells can give different FTIR spectra (46–50), and also that the infrared spectra of the same strain can change when changing the nutrients surrounding it (51). Based on this, there is a potential to use micro-FTIR to discriminate different bacterial populations, without sample preparation, by comparing the FTIR spectra obtained in different areas of the scanned surface, or even the observation of differences between the same strains based on variables such as growth phase or nutrients. The use of algorithms for data analysis, such as principal component analysis (PCA), has been successfully applied to vibrational spectroscopy to allow the identification of key chemical moieties that distinguish between different strains (34–37, 52). The chemical mapping obtained using micro-FTIR allows the discrimination between very small differences in structure, morphology, and chemical content in a bacterial sample, providing vital information about its composition and impurities.

2. Materials

2.1. KBr Pellets

1. Spectroscopic grade potassium bromide.
2. A drying oven capable of reaching 120°C.
3. An evacuable pellet die kit for the preparation of KBr discs is necessary, as shown in Fig. 6. There are several sizes available, but 13 mm is the standard size for FTIR pellets.
4. Hydraulic press, capable of delivering 10 tons pressure.
5. Rotary vacuum pump.
6. Pellet sample holder.
7. A desiccator.

2.2. Transmission Flow Cell

1. A leak-free FTIR transmission demountable liquid cell. Figure 7 shows two examples of commercially available liquid transmission cells
2. A peristaltic or syringe pump capable of delivering low flow rates (around 3 mL/h).

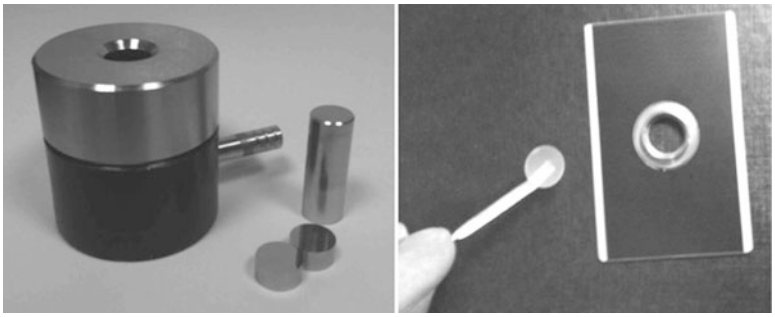

Fig. 6. Evacuable pellet die kit for the preparation of KBr pellets (*left*), and a typical 11-mm diameter KBr pellet, next to a pellet holder for transmission measurements (*right*).

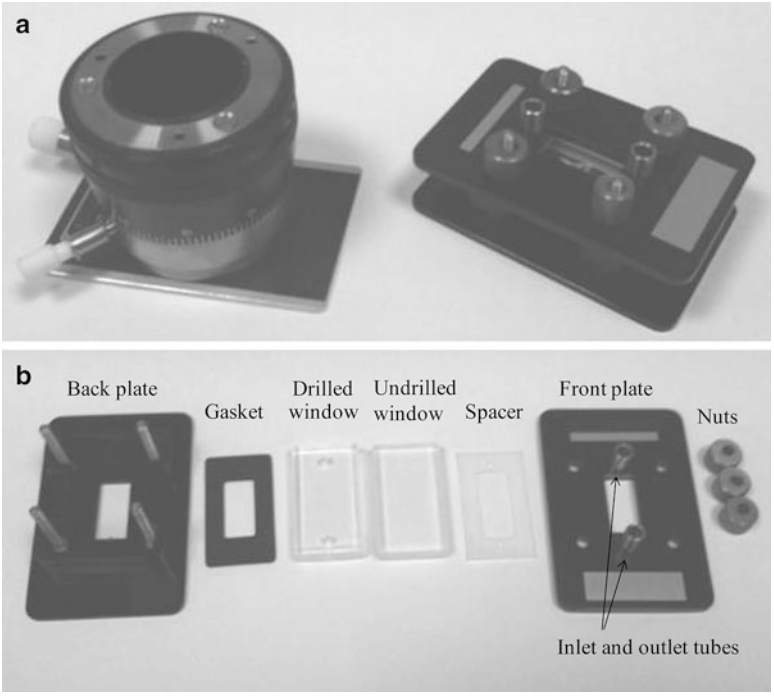

Fig. 7. FTIR transmission liquid cells. (**a**) Two commercially available liquid cells: The variable path length liquid cell with circular windows (*left*) allows continuous adjustment of sample path length using a micrometer scale marked on the cell body. The rectangular liquid transmission cell (*right) uses spacers of various thicknesses to vary the cell path length. (b) Demounted rectangular* liquid cell with its components.

2.3. Attenuated Total Reflectance-Fourier Transform Infrared Spectroscopy

1. Adequate ATR-FTIR accessory, compatible to the FTIR spectrometer in use.

2.4. Micro-FTIR Studies

For reflectance micro-FTIR spectroscopy:

1. A highly reflective surface, for background correction. This highly reflective surface is usually a gold-coated mirror, and is commonly included with the FTIR microscope.

For transmitted micro-FTIR spectroscopy:

1. Infrared transparent windows, such as calcium fluoride (CaF_2), barium fluoride (BaF_2), zinc selenide (ZnSe) or sodium chloride (NaCl).
2. Alternatively, a transmission flow cell or KBr pellets (see Note 1).

3. Methods

3.1. KBr Pellets

A KBr pellet is prepared by grinding the freeze-dried bacterial sample with solid KBr and applying pressure to the dry mixture. KBr is chosen because it is transparent to infrared radiation.

In order to analyse bacterial samples by forming KBr discs, the following step should be considered:

1. Before preparing the KBr pellet, the bacterial cells should be freeze-dried (see Note 2).
2. Dry the KBr powder for at least 3 h at 120 C in a suitable oven, and let it to cool in a desiccator.
3. Add approximately 150 mg of KBr and 1 mg of sample to an agate mortar and grind and mix together carefully, taking care not to damage the cells while mixing. Do not mix for very long as the KBr is highly hygroscopic.
4. Assemble the two parts of the die body and insert one of the die pellets with its polished side up.
5. Put the KBr and sample mixture into the die and spread evenly with the plunger (see Note 3). Remove the plunger slowly allowing air to enter the die.
6. Press the second die pellet in the die with its polished side down. Insert the plunger into the die.
7. Place the die into a hydraulic press, connect a vacuum hose to the vacuum port, and evacuate the die (e.g., using a rotary pump) for about 5 min, to dry the sample before applying pressure.
8. After about 5 min of evacuation, apply 8–10 tons of pressure for 3–5 min with the hydraulic press, leave the vacuum on during this step. The maximum pressure that the die can resist will depend on its size and the manufacturer's specifications. However, for most of the 13 mm dies, a maximum of 10 tons may be applied.

9. Switch off the vacuum and gradually release the pressure from the die by opening the bleed screw of the hydraulic press slowly (rapid release of the pressure may crack or break the disk).
10. Remove the die from the hydraulic press. Remove the base of the die, invert it, and hold it inverted, taking care not to let the plunger fall out at the bottom. Push down the upper part of the die body until the lower die pellet drops out of the bore (it may be necessary to use the hydraulic press to force the ram down).
11. Remove the KBr disc from between the die pellets taking care not to scratch the polished pellet surfaces.
12. Using tweezers or a small spatula, transfer the pressed KBr disk to the appropriate disk holder for IR analysis.
13. The sample should be analysed as soon as possible, before it has time to absorb atmospheric moisture.
14. The die body, plunger, and disc pellets should be cleaned with a damp tissue with isopropanol or acetone, using only soft tissues to wipe the polished surfaces as some paper may scratch them, and then stored in a dry place.

3.2. Attenuated Total Reflectance-Fourier Transform Infrared Spectroscopy

There are many manufacturers and ATR accessories, which vary in sensitivity and versatility with different types and sizes of crystals (such as Germanium, Diamond, ZnSe, etc.), and can even include heated top plates, reaction plates or super-critical fluid cells. In general, for bacterial analysis, a basic ATR accessory is more than enough, and any crystal will be adequate for a wide range of analysis at neutral pH values. If the analysis requires the study of extremophile bacteria, for example, that involves measurements at very low pH values (pH around 1 or 2), then a diamond crystal will be more suitable. In addition, if the study involves temperature changes, then a low temperature or heated top plate may be needed.

For the analysis of bacterial cells using ATR-FTIR, the following steps should be performed:

1. The ATR accessory should be aligned according to the manufacturer's instructions. This usually involves adjusting the internal mirrors to maximise the energy reaching the detector. In most cases, however, this alignment procedure is only required when the accessory is installed for the first time.
2. Obtain a background spectrum using the same resolution and the number of accumulations to be used for the sample. The background spectra can be a scan of the empty ATR crystal or the supernatant of centrifuged cell suspensions, for example. In any case, final spectrum should be the result of the sample single beam normalised against the background and consequently, the spectra of the bacterial sample should not include any of the features of the matrix where it is immersed.

3. Carefully, place the bacterial cells on the top of the ATR crystal, ensuring a direct contact between the cells and the crystal. This can be done using a sterile loop, and homogeneously spreading the cells to cover the whole ATR crystal surface. Alternatively, a drop of bacterial suspension can be deposited on top of the ATR crystal.
4. Obtain an infrared spectrum of the sample, following the instructions of the manufacturer's spectrometer, and using the same resolution and accumulation of the background spectra.
5. It should be noted that too much water will mask the bacterial features in the spectra. Therefore, if decent infrared spectra cannot be obtained due to excess of water, it is recommended to let the sample dry until a thin biofilm can be observed on top of the crystal.
6. Moderate vacuum or gentle heating can be applied to dry the sample. Alternatively, leaving the suspension to dry at room temperature or under a gentle gas flow (such as N_2) is also suitable. However, the correct drying method should be chosen according to the inherent characteristic of the sample, ensuring that the properties of the cells under study are not altered.
7. Some ATR-FTIR accessories come with a fixed angle of incidence that cannot be changed. However, if the ATR accessory allows changes in the angle of incidence, this can be adjusted to maximise the intensity of the bands in the spectra. Decreasing the angle of incidence of the infrared beam on the crystal will increase the penetration depth, increasing the intensity of the resulting spectrum. On the other hand, if the sample is producing spectral features in the spectrum that are very intense, the angle of incidence at the crystal could be increased to lower the penetration depth.
8. It is recommended that the sample be removed without scratching the surface of the crystal, as slight scratches on the crystal will result in a reduction in the quality of future spectra. A mild solvent, such as isopropanol, and cotton but could be used to remove the sample.

3.3. Liquid Flow cell

Because water absorption is usually the major challenge when using a liquid flow cell, the optical thickness of water should be minimal, but enough to support life and ensure the validity of the cells. To achieve this, a minimal path length should be selected (by either using a spacer of minimum thickness or by decreasing the path length if an adjustable flow cell is used).

The liquid flow cell could be of fixed or variable path length, and the selection of path lengths can be made using spacers of

different thickness (usually made of mylar, PTFE, or Teflon). The cell windows are usually made of calcium fluoride (CaF_2), barium fluoride (BaF_2), zinc selenide (ZnSe), or other infrared transparent material. The use of sodium chloride (NaCl) windows for biofilm analysis is not recommended because the aqueous media will dissolve the windows. For the analysis of bacteria, a demountable liquid cell is recommended, instead of a permanently mounted cell, because it is much easier to clean afterwards and allows the adjustment of path lengths. Figure 6 shows a demounted liquid flow cell.

1. Assemble the flow cell according to the manufacturer's instructions.
2. The whole flow system should be disinfected with 70% ethanol for 5 h and rinsed with sterile water for 24 h (53).
3. Prior to sample analysis, the flow system should be conditioned by passing distilled water, saline solution, or another suitable medium for the biofilm analysis, using a peristaltic or syringe pump (see Note 4).
4. Obtain a background spectrum of the liquid medium.
5. Inoculation or introduction of the bacterial sample into the flow system must be carried out under sterile conditions, avoiding formation of air bubbles in the flow cell.
6. Monitor the bacterial growth by measuring the absorbance spectra as a function of time (see Note 5) while maintaining a constant flow-rate. Alternatively, the biofilm growth can be studied in static mode, by conditioning the flow system first, then stopping the nutrient supply to the system, removing all tubing, and observing the biofilm growth alone (30).

3.4. Micro-FTIR

Micro-FTIR is a very simple technique and usually requires minimal preparation. Usually, samples can be measured directly or transferred onto an infrared transparent substrate. Micro-FTIR analyses of bacteria can be performed either in transmission or reflectance mode. Transmission mode gives high-quality spectra but requires infrared transparent surfaces and transfer of the colonies from the agar plate (16, 18, 21). Recent advances in detector sensitivity have allowed the use of reflectance micro-FTIR spectroscopy as an important analytical tool to analyse thick opaque surfaces and raw materials without the need of previous treatment.

Previous studies of reflectance micro-FTIR on flat/polished organic samples employed a Kramers-Kronig transformation due to abnormal dispersion resulting from highly specular surfaces (54–56). However, recent studies of bacterial growth on flat surfaces, scanned using reflectance micro-FTIR, did not require this transformation as the band peak positions were the same in the transmission and reflectance mode, and both spectra were not different (17). This could be because, on reflectance mode, the

bacterial samples form a thin biofilm lying on a flat reflective surface, preventing the abnormal dispersion resulting from highly specular surfaces of polished or shiny materials (17).

1. Set-up the FTIR micro-spectrometer according to the manufacturer's instructions. If the micro-FTIR spectrometer is fitted with a Mercury–Cadmium–Telluride detector, fill the detector reservoir with liquid nitrogen before taking measurements.
2. If working on transmission mode, carefully transfer the bacterial cells onto an infrared transparent medium such as KBr pellet or CaF_2 windows. If working in reflectance mode, make sure the bacterial cells are on a relatively flat or polished surface.
3. Position the sample on the microscope stage and generate a focused visible image of the area of interest.
4. Select a suitable aperture for the infrared scans. Current commercial micro-FTIR spectrometers can provide image resolutions of up to 2 μm^2. However, the smaller the aperture size the noisier the spectra, due to less amount of light reaching the detector. An optimal aperture size should be selected depending on the characteristics of the sample and the quality of the spectra produced (see Note 6).
5. Obtain a background spectrum. In case of transmission mode, the substrate where the sample is placed is a suitable background. In reflectance mode, a highly reflective surface is generally used (such as a golden coated mirror, usually provided by the instrument's manufacturer).
6. Draw a box around the area of interest and start the infrared scan. An IR image comprising hundreds or even thousands of spectra will be generated as a false colour visible image. Each pixel will represent an individual spectrum. A "chemical map" can be generated by selecting the functional groups of interest.
7. Depending on the manufacturer's software, it may be possible to perform a principal component analysis to allow the identification of key chemical moieties that distinguish between different regions.
8. If the stage allows it, it could also be possible to analyse KBr pellets or liquid suspensions in a flow cell in transmission mode under the FTIR microscope. The preparation of the pellet or the setting up of the liquid cell is described in the previous sections, and the microanalysis only requires the pellet or liquid cell to be placed on the microscope stage and focused on the optical microscope before generating an infrared map scan. The combination of flow cells and micro-FTIR allows the generation of chemical maps while monitoring changes in situ, for example, changes in bacterial properties when varying parameters such as nutrients or pH, or the developments of biofilms over time.

4. Notes

1. Caution should be taken if using NaCl windows, as these windows will dissolve with aqueous samples; therefore, they should be used only with water-free samples (such as freeze-dried cells).
2. Freeze-drying, also known as lyophilisation, is a process in which frozen material is dried through the sublimation of ice. Several protocols for the freeze-drying of bacterial samples are available in the literature. For example, the reader could consult the references (57, 58).
3. This can be done by rotating the plunger lightly, as the KBr can stick if the plunger is pressed down very hard.
4. The adequate flow rate for the monitoring of biofilms can vary depending on the bacterial strain or application. Flow rates between 3 and 5 mL/h have been reported for soil or oral bacteria (59, 60) whereas flow rates of up to 45 mL/h have been reported for drinking water biofilms (53).
5. The duration of the experiment depends strongly on the type of study of interest and the velocity of the bacterial growth. For example, oral biofilms have been previously monitored for 3 days (59), whereas nascent *Pseudomonas fluorescens* have been studied for 3 h (53). The number of accumulations is also an important parameter to consider. While a high number of scans (>100) is always recommended to improve the signal-to-noise ratio, the time these scans take to be completed should not affect the observation of two subsequent spectral changes in response to other experimental variables.
6. As with all other FTIR techniques, the quality of the spectra is also affected by the number of accumulations and spectral resolution. A higher number of accumulations will produce better signal-to-noise ratio. Decreasing the resolution will produce smoother spectra, but the ability to distinguish between two adjacent bands will be compromised. In general, a resolution of 4 cm^{-1} and accumulations of 100 scans or higher is a good compromise between good spectral quality and low noise.

References

1. Coblentz WW (1911) Radiometric investigation of water of crystallization, light filters and standard absorption bands. Bull Bur Stand 7:619–663
2. Stair R, Coblentz WW (1935) Infrared absorption spectra of plant and animal tissue and of various other substances. J Res Nat Bur Stand 15:295–316
3. Randall HM, Smith DW, Colm AC, Nungester WJ (1951) Correlation of biologic properties of strains of *Mycobacterium* with infra-red spectrums. 1. Reproducibility of extracts of

M-tuberculosis as determined by infra-red spectroscopy. Am Rev Tuberc 63:372–380

4. Randall HM, Smith DW, Nungester WJ (1952) Correlation of biologic properties of strains of *Mycobacterium* with their infrared spectrums. 2. The differentiation of 2 strains, H37Rv and H37Ra, of M-tuberculosis by means of their infrared spectrums. Am Rev Tuberc 65:477–480
5. Randall HM, Smith DW (1953) Infrared spectroscopy in bacteriological research. J Opt Soc Am 43:1086–1092
6. Smith DW, Harrell WK, Randall HM (1954) Correlation of biologic properties of strains of *Mycobacterium* with their infrared spectrums. 3. Differentiation of bovine and human varieties of *M.tuberculosis* by means of their infrared spectrums. Am Rev Tuberc 69:505–510
7. Riddle JW, Kabler PW, Kenner BA, Bordner RH, Rockwood SW, Stevenson HJR (1956) Bacterial identification by infrared spectrophotometry. J Bacteriol 72:593–603
8. Norris KP (1959) Infrared spectroscopy and its application to microbiology. J Hyg (Lond) 57:326–345
9. Burgula Y, Khali D, Kim S, Krishnan SS, Cousin MA, Gore JP, Reuhs BL, Mauer LJ (2007) Review of mid-infrared Fourier transform-infrared spectroscopy applications for bacterial detection. J Rapid Meth Autom Microbiol 15:146–175
10. Naumann D, Helm D, Labischinski H (1991) Microbiological characterizations by FT-IR spectroscopy. Nature 351:81–82
11. Nichols PD, Henson JM, Guckert JB, Nivens DE, White DC (1985) Fourier transform-infrared spectroscopic methods for microbial ecology: analysis of bacteria, bacteria-polymer mixtures and biofilms. J Microbiol Methods 4:79–94
12. Naumann D (2000) Infrared spectroscopy in microbiology. In: Meyers RA (ed) Encyclopedia of analytical chemistry: applications, theory, and instrumentation. Wiley, Chichester, pp 102–131
13. Naumann D, Helm D, Labischinski H, Giesbrecht P (1991) The characterization of microorganisms by Fourier-transform infrared spectroscopy (FT-IR). In: Nelson WH (ed) Modern techniques for rapid microbiological analysis. VCH, New York, pp 43–96
14. Koenig JL, Wang S-Q, Bhargava R (2001) Peer reviewed: FTIR images. Anal Chem 73:360–369
15. Maquelin K, Kirschner C, Choo-Smith LP, van den Braak N, Endtz HP, Naumann D, Puppels GJ (2002) Identification of medically relevant microorganisms by vibrational spectroscopy. J Microbiol Methods 51:255–271
16. Mossoba MM, Al-Khaldi SF, Kirkwood J, Fry FS, Sedman J, Ismail AA (2005) Printing microarrays of bacteria for identification by infrared micro spectroscopy. Vib Spectrosc 38:229–235
17. Ojeda JJ, Romero-Gonzalez ME, Banwart SA (2009) Analysis of bacteria on steel surfaces using reflectance micro-Fourier transform infrared spectroscopy. Anal Chem 81:6467–6473
18. Orsini F, Ami D, Villa AM, Sala G, Bellotti MG, Doglia SM (2000) FT-IR microspectroscopy for microbiological studies. J Microbiol Methods 42:17
19. Stehfest K, Toepel J, Wilhelm C (2005) The application of micro-FTIR spectroscopy to analyze nutrient stress-related changes in biomass composition of phytoplankton algae. Plant Physiol Biochem 43:717–726
20. Wenning M, Seiler H, Scherer S (2002) Fourier-transform infrared microspectroscopy, a novel and rapid tool for identification of yeasts. Appl Environ Microbiol 68:4717–4721
21. Wenning M, Theilmann V, Scherer S (2006) Rapid analysis of two food-borne microbial communities at the species level by Fourier-transform infrared microspectroscopy. Environ Microbiol 8:848–857
22. Skoog DA, Leary JJ (1992) Principles of instrumental analysis. Saunders College, Philadelphia
23. Coates J (2006) Interpretation of Infrared Spectra, A Practical Approach. Encyclopedia of Analytical Chemistry. Wiley
24. Conley RT (1972) Infrared Spectroscopy. Allyn and Bacon, Boston
25. Dittrich M, Sibler S (2005) Cell surface groups of two picocyanobacteria strains studied by zeta potential investigations, potentiometric titration, and infrared spectroscopy. J Colloid Interface Sci 286:487–495
26. Jiang W, Saxena A, Song B, Ward BB, Beveridge TJ, Myneni SCB (2004) Elucidation of functional groups on gram-positive and gram-negative bacterial surfaces using infrared spectroscopy. Langmuir 20:11433–11442
27. Ojeda JJ, Romero-Gonzalez ME, Bachmann RT, Edyvean RGJ, Banwart SA (2008) Characterization of the cell surface and cell wall chemistry of drinking water bacteria by combining XPS, FTIR spectroscopy, modeling, and potentiometric titrations. Langmuir 24:4032–4040
28. Wade LG (1995) Organic Chemistry. Prentice-Hall, New Jersey

29. Mariey L, Signolle JP, Amiel C, Travert J (2001) Discrimination, classification, identification of microorganisms using FTIR spectroscopy and chemometrics. Vib Spectrosc 26:151–159
30. Schmitt J, Flemming HC (1998) FTIR-spectroscopy in microbial and material analysis. Int Biodeterior Biodegrad 41:1–11
31. Yee N, Benning LG, Phoenix VR, Ferris FG (2004) Characterization of metal-cyanobacteria sorption reactions: A combined macroscopic and infrared spectroscopic investigation. Environ Sci Technol 38:775–782
32. Smith BC (1996) Fundamentals of Fourier transform infrared spectroscopy. CRC, Boca Raton
33. De la Cruz C (2000) Caracterización por FTIR de metales soportados. In: Taller de Caracterización Básica de Materiales Catalíticos y Adsorbentes. Mérida, Venezuela: CYTED-CONICIT
34. Al-Qadiri HM, Al-Holy MA, Lin M, Alami NI, Cavinato AG, Rasco BA (2006) Rapid detection and identification of *Pseudomonas aeruginosa* and *Escherichia coli* as pure and mixed cultures in bottled drinking water using Fourier transform infrared spectroscopy and multivariate analysis. J Agric Food Chem 54:5749–5754
35. Harz A, Rosch P, Popp J (2009) Vibrational spectroscopy-a powerful tool for the rapid identification of microbial cells at the single-cell level. Cytometry A 75A:104–113
36. Huang WE, Hopper D, Goodacre R, Beckmann M, Singer A, Draper J (2006) Rapid characterization of microbial biodegradation pathways by FT-IR spectroscopy. J Microbiol Methods 67:273–280
37. Krafft C, Steiner G, Beleites C, Salzer R (2009) Disease recognition by infrared and Raman spectroscopy. J Biophotonics 2:13–28
38. Goodacre R, Timmins EM, Rooney PJ, Rowland JJ, Kell DB (1996) Rapid identification of *Streptococcus* and *Enterococcus* species using diffuse reflectance-absorbance Fourier transform infrared spectroscopy and artificial neural networks. FEMS Microbiol Lett 140:233–239
39. Naumann D, Keller S, Helm D, Schultz C, Schrader B (1995) FT-IR spectroscopy and FT-Raman spectroscopy are powerful analytical tools for the non-invasive characterization of intact microbial cells. J Mol Struct 347:399–405
40. Busalmen JP, de Sanchez SR, Schiffrin DJ (1998) Ellipsometric measurement of bacterial films at metal-electrolyte interfaces. Appl Environ Microbiol 64:3690–3697
41. Beveridge TJ (1981) Ultrastructure, chemistry, and function of the bacterial wall. Int Rev Cytol 72:229–317
42. Bouhedja W, Sockalingum GD, Pina P, Allouch P, Bloy C, Labia R, Millot JM, Manfait M (1997) ATR-FTIR spectroscopic investigation of E. coli transconjugants [beta]-lactams-resistance phenotype. FEBS Lett 412:39–42
43. Holman H-YN, Miles R, Hao Z, Wozei E, Anderson LM, Yang H (2009) Real-time chemical imaging of bacterial activity in biofilms using open-channel microfluidics and synchrotron FTIR spectromicroscopy. Anal Chem 81:8564–8570
44. Moss DA, Keese M, Pepperkok R (2005) IR microspectroscopy of live cells. Vib Spectrosc 38:185–191
45. Beech IB (2004) Corrosion of technical materials in the presence of biofilms—current understanding and state-of-the art methods of study. Int Biodeterior Biodegrad 53:177–183
46. Bosch A, Minan A, Vescina C, Degrossi J, Gatti B, Montanaro P, Messina M, Franco M, Vay C, Schmitt J, Naumann D, Yantorno O (2008) Fourier transform infrared spectroscopy for rapid identification of nonfermenting gram-negative bacteria isolated from sputum samples from cystic fibrosis patients. J Clin Microbiol 46:2535–2546
47. Curk MC, Peladan F, Hubert JC (1994) Fourier-transform infrared (FTIR) spectroscopy for identifying *Lactobacillus* species. FEMS Microbiol Lett 123:241–248
48. Garip S, Gozen AC, Severcan F (2009) Use of Fourier transform infrared spectroscopy for rapid comparative analysis of Bacillus and Micrococcus isolates. Food Chem 113:1301–1307
49. Kirschner C, Maquelin K, Pina P, Thi NAN, Choo-Smith LP, Sockalingum GD, Sandt C, Ami D, Orsini F, Doglia SM, Allouch P, Mainfait M, Puppels GJ, Naumann D (2001) Classification and identification of enterococci: a comparative phenotypic, genotypic, and vibrational spectroscopic study. J Clin Microbiol 39:1763–1770
50. Savic D, Jokovic N, Topisirovic L (2008) Multivariate statistical methods for discrimination of lactobacilli based on their FTIR spectra. Dairy Sci Technol 88:273–290
51. Eboigbodin KE, Ojeda JJ, Biggs CA (2007) Investigating the surface properties of *Escherichia coli* under glucose controlled conditions and its effect on aggregation. Langmuir 23:6691–6697
52. Huang WE, Griffiths RI, Thompson IP, Bailey MJ, Whiteley AS (2004) Raman microscopic

analysis of single microbial cells. Anal Chem 76:4452–4458

53. Delille A, Quiles F, Humbert F (2007) In situ monitoring of the nascent *Pseudomonas fluorescens* biofilm response to variations in the dissolved organic carbon level in low-nutrient water by attenuated total reflectance-Fourier transform infrared spectroscopy. Appl Environ Microbiol 73:5782–5788
54. Hacura A, Wrzalik R, Matuszewska A (2003) Application of reflectance micro-infrared spectroscopy in coal structure studies. Anal Bioanal Chem 375:324–326
55. Mastalerz M, Bustin RM (1995) Application of reflectance micro-Fourier transform-infrared spectrometry in studying coal macerals—comparison with other Fourier-transform infrared techniques. Fuel 74:536–542
56. Mastalerz M, Bustin RM (1996) Application of reflectance micro-Fourier transform infrared analysis to the study of coal macerals: an example from the Late Jurassic to Early Cretaceous coals of the Mist Mountain Formation, British Columbia, Canada. Int J Coal Geol 32:55–67
57. Perry SF (1998) Freeze-drying and cryopreservation of bacteria. Mol Biotechnol 9:59–64
58. Sourek J (1974) Long-term preservation by freeze-drying of pathogenic bacteria of Czechoslovak National Collection of Type Cultures. Int J Syst Bacteriol 24:358–365
59. Landa AS, van der Mei HC, Busscher HJ (1997) Detachment of linking film bacteria from enamel surfaces by oral rinses and penetration of sodium lauryl sulphate through an artificial oral biofilm. Adv Dent Res 11:528–538
60. Ojeda JJ, Romero-Gonzalez ME, Pouran HM, Banwart SA (2008) In situ monitoring of the biofilm formation of *Pseudomonas putida* on hematite using flow-cell ATR-FTIR spectroscopy to investigate the formation of inner-sphere bonds between the bacteria and the mineral. Mineral Mag 72:101–106